ISBN: 978-3-95450-132-8 doi:10.18429/JACoW-IPAC2014-TUYB01

VERTICAL ORBIT-EXCURSION FIXED FIELD ALTERNATING GRADIENT ACCELERATORS (V-FFAGs) AND 3D CYCLOTRONS

S.J. Brooks*, BNL, Upton, NY 11973, USA

Abstract

FFAGs with vertical orbit excursion (VFFAGs) provide a promising alternative design for rings with fixed-field (e.g. superconducting) magnets. They have a vertical magnetic field component that increases with height in the vertical aperture, yielding a skew quadrupole focussing structure. Scaling type VFFAGs have fixed tunes and no intrinsic limitation on momentum range; they are also isochronous in the ultra-relativistic limit. Extending isochronism to lower velocities requires a slanted orbit excursion: a three-dimensional analogue of a spiral sector cyclotron from 40 to 1500 MeV is developed, which is flat at low energies and acquires a slope as the protons become relativistic. This provides more stable tunes than a comparable planar cyclotron. Such machines are promising future candidates for nuclear transmutation using high average power CW beams at ~GeV energies.

PURE VERTICAL ORBIT EXCURSION

In a fixed-field ring accelerator such as a cyclotron or FFAG, the closed orbit will move during acceleration to the point where the integrated bending field satisfies $\oint B_y \, \mathrm{d}s = 2\pi p/q$, which closes a full turn at momentum p. This assumes the acceleration is adiabatic and the optics are linearly stable, in which case the problem is conceptually equivalent to moving a pendulum by its string slowly enough that negligible oscillation is acquired. The closed orbit need not move outwards with increasing energy since focussing rather than 'centrifugal force' is responsible for its motion.

In VFFAGs, the orbits move upwards with energy and B_y increases with y. The situation $B_y = B_0 \mathrm{e}^{ky}$ is particularly interesting since the optics obey a scaling law: an increase of momentum $p_0 \to p_1$ shifts all particle orbits upwards by $\Delta y = \frac{1}{k} \ln \frac{p_1}{p_0}$. In the interior of a long magnet, this requires the 2D field shown in Figure 1.

Because the scaling law only involves translation, the optics and machine tunes are also fixed with energy. A ring based on this was investigated in [1] and achieved alternating gradient focussing using the skew quadrupole component of Figure 1's field by making B_0 negative in every second magnet. Unfortunately this also alternated the sign of the dipole bending field and made the ring magnetically inefficient, much as is the case with scaling FFAGs.

Large edge angles can also be used to obtain alternating gradient focussing in a VFFAG [2] (the edge angles and magnet aperture are vertical), while the body of the magnet continues to bend in the same direction. This improved the magnetic efficiency and gave the ring in Figure 2. The scaling law now rotates the orbits about the ring centre slightly as well as translating upwards but the tunes remain fixed.

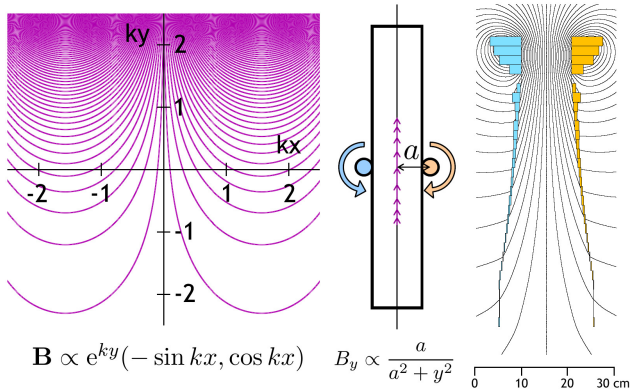

Figure 1: (left) Ideal exponential scaling VFFAG field in 2D; (centre) how to produce vertical field in a vertical aperture with opposing windings; (right) implementation of the VFFAG field with block conductors, from [1].

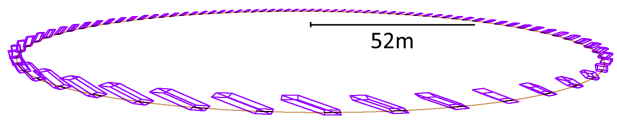

Figure 2: Perspective view of the 12 GeV proton VFFAG with edge angles from [2].

ISOCHRONOUS MACHINES

The circumferences of orbits in VFFAGs (with or without edge focussing) remain constant with energy. This means that for ultra-relativistic beams, they become isochronous and fixed-frequency RF and CW acceleration can be used. This was the approach suggested in one of the earliest papers discussing VFFAGs [3] for electron acceleration.

The velocity of proton beams changes significantly between pre-injector and ~GeV energies. Isochronous cyclotrons conventionally make $\langle B_y \rangle = B_0\gamma$, giving perfect isochronism if the orbit shapes remain similar and scaled by β. Unfortunately at high energies, β and the orbit radius are bounded while γ and the dipole field tend to infinity. The increase in dipole with radius produces a focussing quadrupole proportional to $\frac{\mathrm{d}\gamma}{\mathrm{d}\beta} = \beta\gamma^3$, which increases faster than the $\beta\gamma$ dependence of momentum, so eventually over-focusses the beam. Adding more sectors to get more edge defocussing can give an arbitrarily high maximum energy but for a fixed number of sectors there is always an energy limit.

This over-focussing may be avoided if vertical orbit excursion is introduced at higher energies ([2] §V.B) so that fields for increasing γ are no longer so close together. If the orbit excursion makes an angle of θ with the horizontal, while the **B** field is vertical and increasing with energy, then there is a

* sbrooks@bnl.gov

ISBN: 978-3-95450-132-8 doi:10.18429/JACoW-IPAC2014-TUYB01

$\theta/2$ rotation of the quadrupole. A vertical excursion proportional to $\ln\gamma$ would make the gradient at most proportional to γ, so the optical quadrupole strength would be bounded: this is the scaling VFFAG of the previous section.

3D CYCLOTRON FIELD MODEL

While Maxwellian field models for planar cyclotrons can be found by defining B_y at $y = 0$ and then using the technique in [4] to get a Taylor series for the field at $y \neq 0$, the corresponding method for a 3D cyclotron is more involved. It is summarised below: see [5] for full mathematical details.

Field Extrapolation from a Curved Surface

If $\mathbf{B}$ is defined at a reference surface $y = Y(x,z)$, define a shifted magnetic field $\mathbf{C}(x,y,z) = \mathbf{B}(x,Y(x,z)+y,z)$ so that $\mathbf{C}(x,0,z)$ is the initial condition. Transforming Maxwell's equations in free space to act on $\mathbf{C}$ gives

$$\partial_y \mathbf{C} = \begin{bmatrix} 1 & Y_x & 0 \\ -Y_x & 1 & -Y_z \\ 0 & Y_z & 1 \end{bmatrix}^{-1} \begin{bmatrix} 0 & \partial_x & 0 \\ -\partial_x & 0 & -\partial_z \\ 0 & \partial_z & 0 \end{bmatrix} \mathbf{C},$$

where Y_x and Y_z are partial derivatives of Y. There is also a consistency condition $\partial_z C_x - \partial_x C_z = Y_z \partial_x C_y - Y_x \partial_z C_y$, which was not a difficulty when $Y = 0$ since it could be satisfied by setting $B_x = B_z = 0$ on the mid-plane, but now has a non-trivial effect. It is satisfied ([5] §3.4) by adding particular B_x and B_z components to the initial condition, determined by integrating the desired B_y along a line from the centre of the cyclotron. The field is evaluated via the truncated Taylor expansion

$$\mathbf{B}_N(x,y,z) = \sum_{n=0}^{N} \frac{(y - Y(x,z))^n}{n!} \partial_y^n \mathbf{C}(x,0,z),$$

which is analogous to the planar method except the form of $\partial_y^n \mathbf{C}$ is now extremely complicated and for this paper was evaluated using a computer algebra system.

Spiral Sector Fields

Projecting the shape of the cyclotron onto the x-z plane, the sectors make a constant edge angle θ_e with the radial direction. In polar coordinates (r,θ), a new angular coordinate $\eta = \theta - (\tan\theta_e)\ln r$ has the property that lines of constant η are parallel to the sector edges. Thus the vertical field on the cyclotron's reference plane is set to be

$$B_y(x,Y(x,z),z) = B_0 \gamma g(\eta) = \frac{B_0}{\sqrt{1-(r/R)^2}}\, g(\eta),$$

where γ is the ideal value based on the radius $r = \sqrt{x^2+z^2}$ and the asymptotic radius R corresponding to $\beta = 1$. For the orbits to close, the value $B_0 = mc/qR$ must be chosen for the particle of interest and the function $g(\eta)$, which determines the azimuthal field flutter, should satisfy $\langle g(\eta)\rangle = 1$.

In this paper, $g(\eta)$ is a sum of functions of the form $\pm\tanh((\eta - \eta_n)/\theta_f)$ for sector edge locations η_n that is rescaled to average unity. The value θ_f determines the fringe field extent. The 'packing factor' or proportion of ring taken by the interior of the sectors can also be varied.

Magnet Windings

It is envisioned that the field can be produced in practice by superconducting windings at $y = Y(x,z) \pm \Delta y$ above and below the midplane. This is already a standard arrangement for producing B_y in wide-aperture superconducting dipoles (iron may also be used when B_y dominates). The windings needed for transverse fields have currents that run in opposing directions on either side of the plane rather than symmetrically, like the centre part of Figure 1. Once these current components are added together, winding configurations for above and below should result.

3D CYCLOTRON CLOSED ORBITS

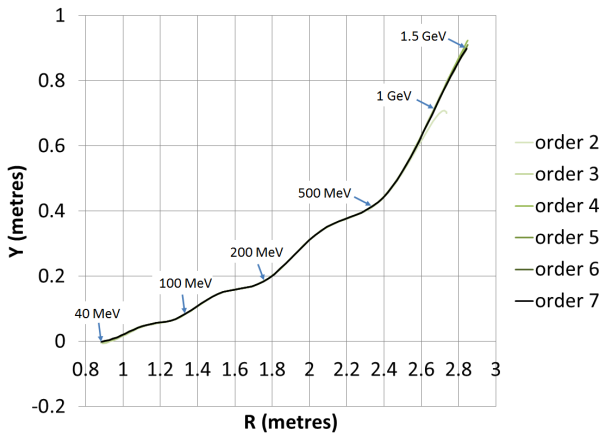

Figure 3: Closed orbit start points in the 3D cyclotron, for magnetic fields evaluated to orders 2 through 7.

Closed orbits for the 3D cyclotron specified in Table 1 were calculated using the Muon1 code ([6], chapter 2). The reference height is given as a function of the ideal $\beta = r/R$ and the azimuthal modulation resulting from the large fringe extent is shown in Figure 4. The orbit positions shown in Figure 3 are at the entrance and exit of a 36° wedge that does not follow the spiral shape, hence the undulations. Figure 13 shows a three-dimensional view of the orbits.

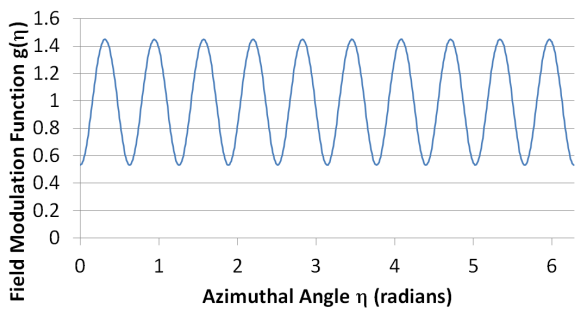

Figure 4: Azimuthal field modulation in the 3D cyclotron.

ISBN: 978-3-95450-132-8 doi:10.18429/JACoW-IPAC2014-TUYB01

Table 1: Parameters of the 3D Cyclotron

Energy range	40–1500	MeV
Radius range	0.8833–2.8738	m
Height range	−0.0023–0.9017	m
Maximum field on orbit	6.747	T
Revolution frequency	15.364±0.096	MHz
Sectors	10	
Sector edge angle θ_e	−63.43	°
Packing factor	54.35	%
Fringe extent θ_f	9.35	°
Mean field (γ=1) B_0	−1	T
Asymptotic radius R	3.1297	m
Reference height $Y(\beta)$ = $0.5324\beta^2 + 1.3168\beta^4 - 2.7235\beta^6 + 2.6954\beta^8$		m
Ring eigentune ranges		
Q_1	1.077–3.531	
Q_2	0.802–1.430	
Q_1 (≥500 MeV)	3.273–3.531	
Q_2 (≥500 MeV)	1.230–1.430	

B_r components in the sector edge fields cause vertical undulations in the orbits. The high energy orbits are also significantly below the theoretical location $r = \beta R, Y = Y(\beta)$, as shown in Figure 5. This is not yet understood and specifying a different initial condition may better align the orbits with the reference surface. The large offset means many terms in the Taylor expansion are needed for convergence, which is why Figure 3 and others show the results converging with each order. Higher orders take exponentially longer to calculate in the current implementation of the field model, limiting how far the series can go.

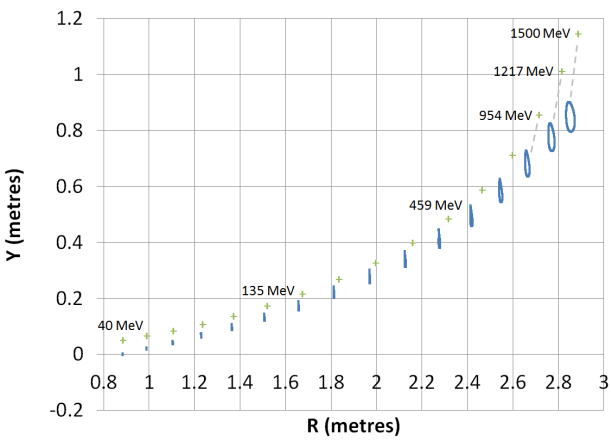

Figure 5: Motion of closed orbit (blue loops) relative to theoretical location on the reference plane (green crosses).

The time of flight shown in Figure 6 varies slightly (±0.62%) because the orbits are not exactly similar in shape. It is hoped that adding a small polynomial $\delta f(\gamma)$ to the overall $B_0\gamma$ field dependence can fine-tune the orbit radii in future. The largest fields encountered at the closed orbits for each energy are shown in Figure 7.

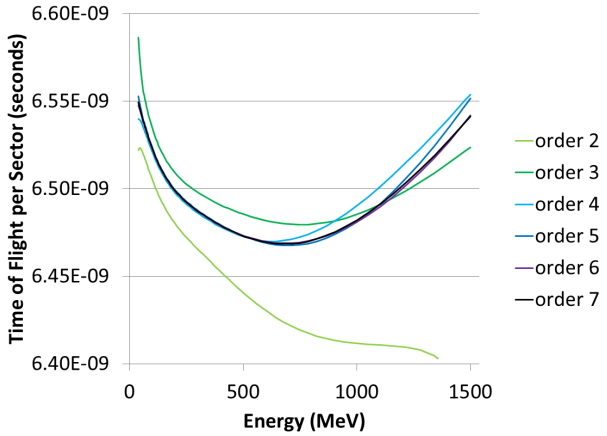

Figure 6: Time of flight per sector of the 3D cyclotron.

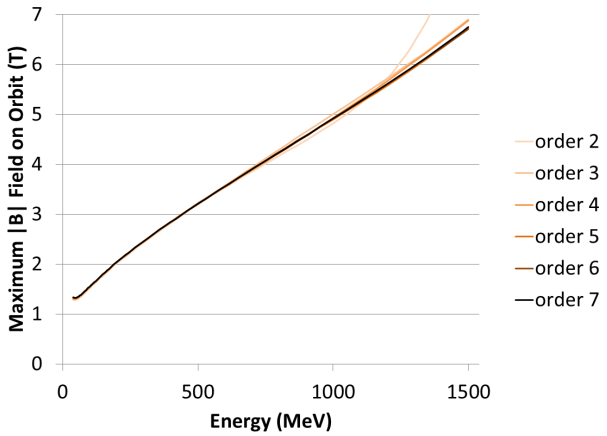

Figure 7: Maximum |**B**| encountered in the 3D cyclotron.

Linear Optics

The tunes per sector of the machine are shown in Figure 8; since the dynamics is coupled, these are 'eigentunes' derived from eigenvalues of the transfer matrix. Above 500 MeV they are reasonably flat, nearly avoiding the half-integer resonances of the 10 sector ring out to 1.5 GeV. The edge angle θ_e was not allowed to vary with energy, which is an important parameter in controlling the tunes in such machines as the TRIUMF cyclotron, so it is expected that better behaviour can be obtained once this is optimised.

Figure 9 shows the two focussing 'eigenplanes' varying with energy, one associated with each eigentune. The behaviour changes from orthogonal planes to skew and back, before ending with a somewhat coupled skew system.

At present, estimation of dynamic aperture is difficult since repeated tracking through the fields amplifies non-symplectic behaviour from the truncated series.

ISBN: 978-3-95450-132-8 doi:10.18429/JACoW-IPAC2014-TUYB01

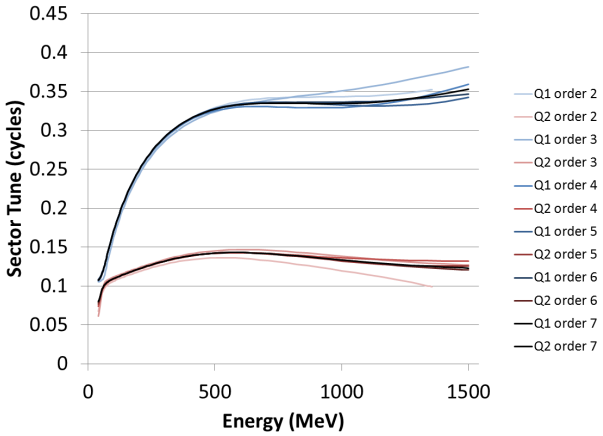

Figure 8: Sector eigentunes of the 3D cyclotron.

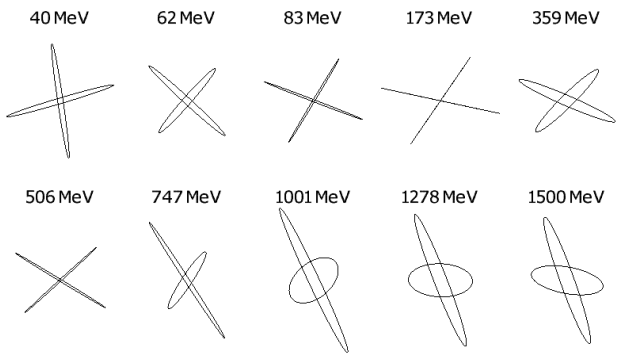

Figure 9: The two linear focussing eigenplanes projected into x-y space for various 3D cyclotron closed orbits.

COMPARISON TO 2D CYCLOTRON

Table 2: Parameters of the Planar Cyclotron

Energy range	40–1500	MeV
Radius range	0.8684–2.9032	m
Maximum field on orbit	6.690	T
Revolution frequency	15.323±0.017	MHz
Sectors	10	
Sector edge angle θ_e	−63.43	°
Packing factor	10.21	%
Fringe extent θ_f	7.04	°
Mean field (γ=1) B_0	−1	T
Asymptotic radius R	3.1297	m
Ring tune ranges		
Q_x	1.096–2.864	
Q_y	0.551–2.594	
Q_x (≥500 MeV)	1.621–2.864	
Q_y (≥500 MeV)	0.551–2.280	

During optimisation studies, entirely planar cyclotrons capable of 1.5 GeV were also found. The cyclotron specified in Table 2 with azimuthal variation shown in Figure 10 produced the orbits shown in Figure 11.

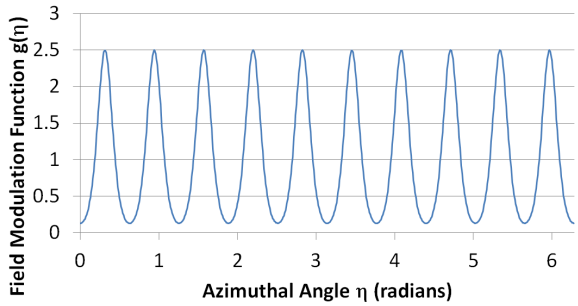

Figure 10: Field modulation in the planar cyclotron.

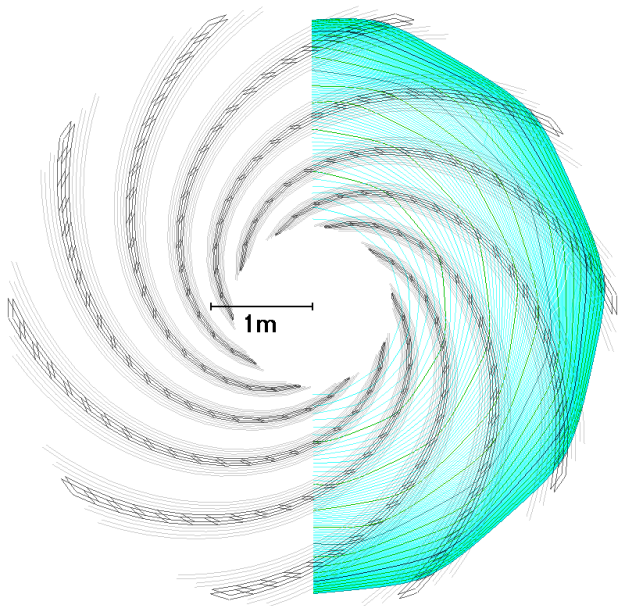

Figure 11: Closed orbits in the planar cyclotron.

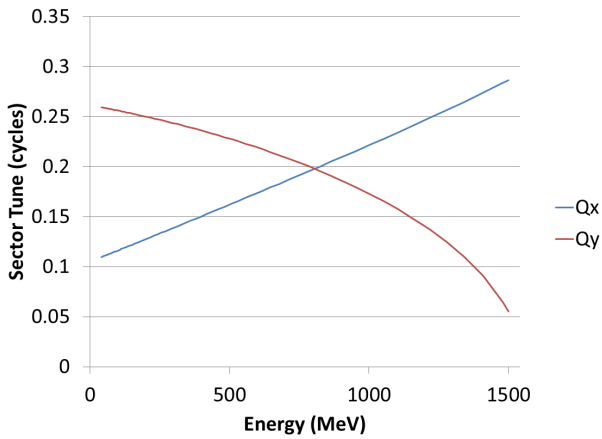

Figure 12: Sector tune variation in the planar cyclotron.

The tunes of this machine (Figure 12) behave very differently to the 3D cyclotron. Q_x must always increase with energy due to the quadrupole from the planar isochronous field, eventually reaching the edge of the stable area with $Q_y = 0$. Many half-integer ring resonances are crossed.

ISBN: 978-3-95450-132-8 doi:10.18429/JACoW-IPAC2014-TUYB01

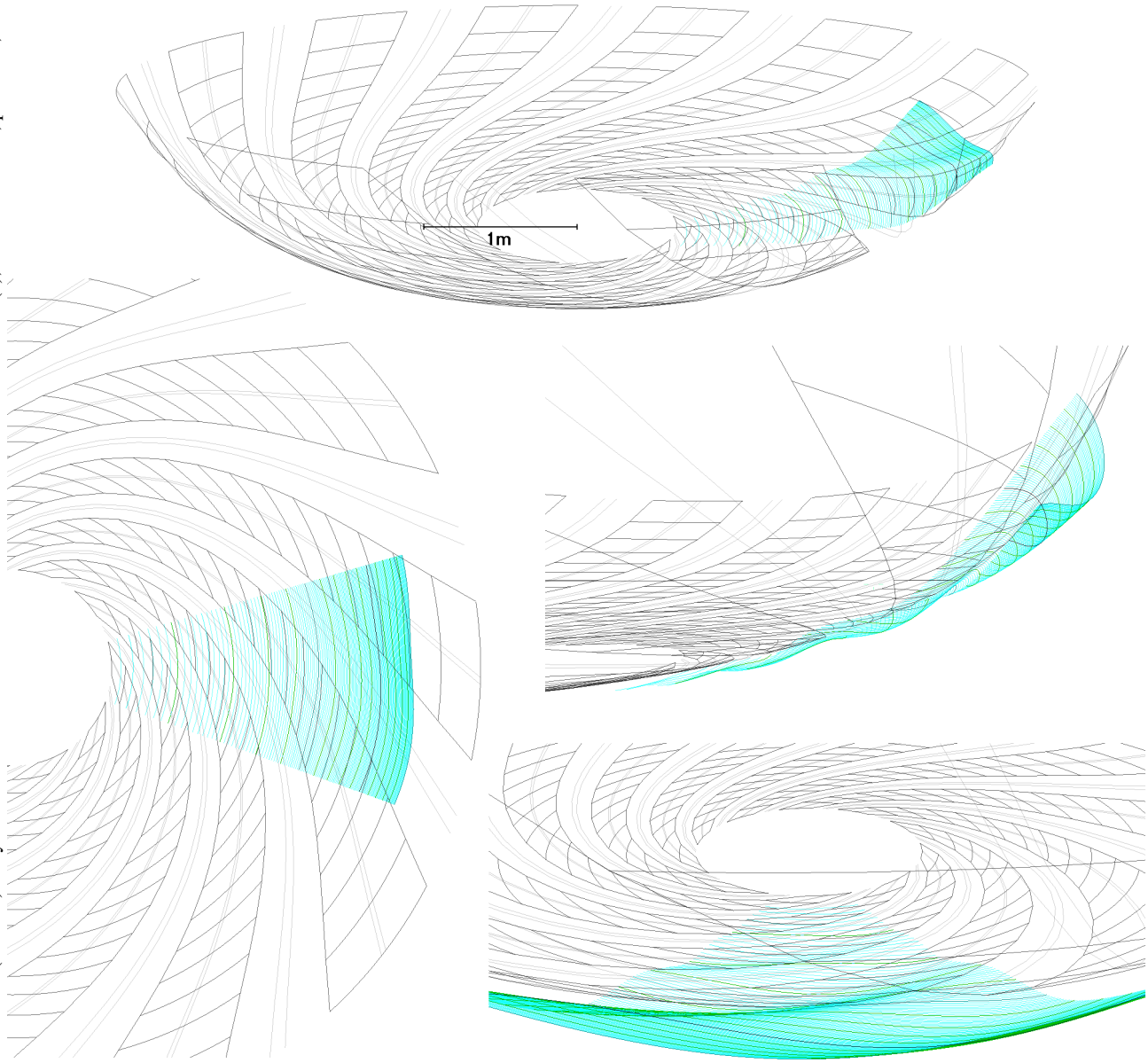

Figure 13: Geometry and closed orbits of the 3D cyclotron in plan view (left) and various perspective views, showing orbit undulation and downward offset of orbits from the reference plane (centre right).

CONCLUSION AND FUTURE WORK

3D cyclotrons promise cyclotron-like performance above 1 GeV, where there are high cross sections for spallation reactions. They were first successfully tracked only a month before IPAC'14, so many tasks still need to be addressed:

- Better alignment between the reference plane and the orbits, giving better convergence in the field model and enabling dynamic aperture calculations;
- Field adjustments to improve isochronism from the current ±0.62% variation;
- Vary θ_e with energy to improve tune control;
- Make space for RF by using fewer sectors and/or more field-free space between sectors;
- Find an example superconducting winding scheme;
- Build scaled-down electron model of the 3D cyclotron.

REFERENCES

[1] *Vertical Orbit Excursion FFAGs*, S.J. Brooks, Proc. HB2010.

[2] *Vertical Orbit Excursion Fixed Field Alternating Gradient Accelerators*, S.J. Brooks, Phys. Rev. ST Accel. Beams 16, 084001 (2013).

[3] *Accelerators with Vertically Increasing Field*, J. Teichmann, Atomnaya Énergiya 12(6), 475 (1962).

[4] *Extending the Energy Range of 50 Hz Proton FFAGs*, S.J. Brooks, Proc. PAC'09, FR5PFP025.

[5] *Extrapolation of Magnetic Fields from a Curved Surface*, S.J. Brooks, note available from `http://stephenbrooks.org/ap/report/2014-2/offsurface.pdf` (2014).

[6] *Muon Capture Schemes for the Neutrino Factory*, Stephen Brooks, D.Phil., University of Oxford, available from `http://ora.ox.ac.uk/objects/ora:4360` (2010).